

# Frequency Factor and Energy Distribution of Shallow Traps in Cadmium Sulfide\*

JAMES J. BROPHY AND ROBERT J. ROBINSON  
*Physics Division, Armour Research Foundation, Chicago, Illinois*

(Received December 10, 1959)

Current noise and photoconductivity measurements taken under uniform 5200 Å illumination on CdS single crystals are used to derive the energy distribution and frequency factor of shallow traps in the range 0.3 to 0.6 electron volt below the conduction band for samples of different CuCl impurity content. Trap densities varying from  $10^{12}$  to  $10^{17}$  cm<sup>-3</sup> ev<sup>-1</sup> and total trap concentrations of  $10^{16}$  cm<sup>-3</sup> with discrete levels at 0.36, 0.43, and 0.60 ev below the conduction band are observed. In a moderately doped, good photo-sensitive crystal, the traps also have a continuous distribution in energy and all have the same frequency factor,  $10^{11}$  sec<sup>-1</sup>, which suggests the traps are structurally similar. The results imply that a photoelectron may experience several thousand retrapping transitions on the average before recombining. It is possible to account semiquantitatively for the  $1/f$  noise spectrum observed in some crystals at high frequencies in terms of the near exponential trap distributions and constant frequency factor derived from low-frequency noise measurements.

## I. INTRODUCTION

THE photoconductive properties of cadmium sulfide are known to be a sensitive function of the nature and distribution of trap levels in the forbidden band.<sup>1</sup> Information about these levels has been derived from such measurements as photoconductivity, thermally stimulated currents, space-charge limited currents, and thermoluminescence. However, many details of the trapping kinetics are not yet well understood. This paper reports results of coupled photoconductivity and current noise measurements on CdS which provide new information about these processes.

Electrical noise in CdS has been previously reported<sup>2</sup> and analyzed<sup>3</sup> in terms of trapping transitions. Here we attempt to extend these ideas and derive a more detailed understanding about electronic transition probabilities between the conduction band and shallow trapping states. Electrical current noise measurements are particularly suitable for this since the noise is due to fluctuations in the number of conduction electrons, and trapping transitions cause such fluctuations. Furthermore, the measurements are made under steady-state conditions in contrast to temperature drift experiments conventionally used to derive trap escape probabilities in insulating solids.

Current fluctuations in single crystals of CdS are determined under uniform, monochromatic illumination of wavelength near the photoconductive peak. The photoelectrons in the conduction band experience trapping and retrapping in levels near the conduction band and finally disappear through recombination to deeper lying states. The observed current fluctuations are a measure of these effects. Variation of illumination intensity sweeps the quasi-Fermi level through the trap level distribution, thus altering the contribution of the various states. Throughout the work it is assumed that

the trap levels examined are simple traps and that they are in thermal equilibrium with the electrons in the conduction band.

The current noise results coupled with density of states data yield a description of the trap escape probabilities and the average number of times a conduction electron is trapped before recombining. Furthermore, this description is capable of predicting fine structure in the noise spectra which is in agreement with observations.

## II. EXPERIMENTAL TECHNIQUE

The specimens studied were single crystals produced by the standard vapor phase technique, CuCl doped during growth, and several millimeters in the largest dimension as shown in Table I. Sample *D* was not intentionally doped and grew in the shape of a hexagonal rod while *A*, *B*, and *C* contained increasing amounts of doping and were flat plates. Crystals *B* and *C* came from the same growth batch. The specimens were provided with soldered indium electrodes which proved to be low noise with the exception of those on sample *D*. The spectrum for this crystal exhibited  $1/f$  noise over the entire frequency range, which is attributed to poor contacts. The other specimens showed no low-frequency  $1/f$  noise down to the lowest frequency of interest.

The circuit of Fig. 1 was used for both noise and photoconductivity measurements. Only a single mercury cell supplied the current in order to be certain that

TABLE I. Characteristics of samples.

Sample no.	$l$ cm	$w$ cm	$t$ cm	Gain	Doping
<i>A</i>	0.2	0.2	$3.3 \times 10^{-2}$	30	Moderately doped
<i>B</i>	0.2	0.2	$3 \times 10^{-2}$	25	Lightly doped
<i>C</i>	0.25	0.25	$4 \times 10^{-2}$	1.5	Lightly doped
<i>D</i>	0.2	0.12	0.2	14	Undoped

\* Supported by the Office of Naval Research.

<sup>1</sup> A. Rose, RCA Rev. **12**, 362 (1951).

<sup>2</sup> K. M. Van Vliet et al., Physica **22**, 723 (1956).

<sup>3</sup> K. M. Van Vliet and J. Blok, Physica **22**, 525 (1956).

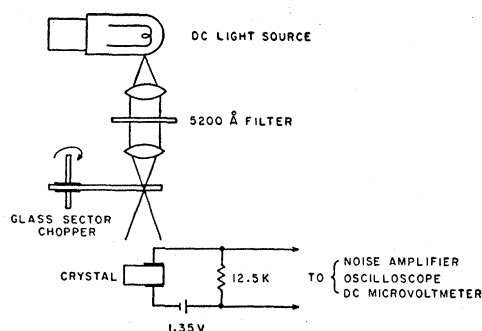


FIG. 1. Sketch of experimental arrangement.

field-induced carrier multiplication effects were negligible. Noise voltages developed across the wirewound load resistor were measured with a straightforward tunable amplifier-voltmeter system giving a true rms indication of the noise voltage. The system was periodically calibrated against the Nyquist noise of known resistors. Noise due to the mercury cell was shown to be negligible by replacing the crystal with wirewound resistors and determining that only Nyquist noise was present.

Illumination was supplied by an 18-ampere tungsten ribbon lamp fed from storage batteries. A 5200 Å interference filter was used exclusively in this work. Except for the 5200 Å radiation, the crystals were otherwise shielded from illumination and were generally kept in the dark when not in use, although no spurious effects from exposure to white light were noticed. For photoconductive decay measurements, the light was chopped at a  $\frac{1}{2}$  second rate by rotating a glass microscope slide through the beam at the focal point. This produced a 4% change in intensity which was sufficient to detect except at the very lowest intensities. Here the glass was replaced by an opaque sector. Intensity of the 5200 Å illumination at the sample position was calibrated with an Eppley thermopile.

The photoconductive decay time  $\tau_0$  was determined with a Tektronix Type 536 oscilloscope connected across the load resistor. Oscilloscope photographs were used to record the traces which were then plotted on semi-logarithmic paper. These plots showed good exponential character and decay times were determined from their slopes. Such measurements were made for illumination intensities yielding dc photocurrents in the range  $10^{-3}$  to  $10^2$  microampere. The photocurrent was determined by measuring the dc voltage drop across the load resistor with a HP 425A microvoltmeter. For each intensity the position of the electron quasi-Fermi level below the conduction band was computed from the sample geometry and resistance, assuming an electron mobility of  $200 \text{ cm}^2/\text{volt-sec}$  and a conduction band density of states of  $10^{19} \text{ cm}^{-3}$ . The variation of  $\tau_0$  with quasi-Fermi level position for each of the crystals is shown in the upper curves of Fig. 2. In general  $\tau_0$  decreases as the quasi-Fermi level rises higher in the forbidden band.

The conduction band lifetime  $\tau_c$  is calculated from the same measurements using the expression  $\tau_c = n_0/n_L$  where  $n_0$  is the conduction band electron concentration determined from the conductivity and  $n_L$  is the rate of production of electron density due to photon absorption. A value for  $n_L$  was obtained from the rate of 5200 Å photons absorbed in the sample and an assumed unity quantum efficiency. The rate comes from calibration of the light source and measurement of sample absorption by determining the intensity of light transmitted through the sample. For these specimens approximately 50% absorption was present, which indicates that photoelectrons are produced reasonably uniformly throughout the crystal. As shown in the lower curves of Fig. 2,  $\tau_c$  tends to approach  $\tau_0$  at higher illumination intensities.

Such measurements may also be used to calculate the photoconductive gain,  $G = (i/e)/n_L V$ , where  $i$  is the photocurrent,  $e$  the electronic charge, and  $V$  the sample volume. The calculated gains in Table I show that crystal A is most sensitive, which was expected from the approximate CuCl concentration. These gains are much lower than those usually quoted in the literature due to the very low applied voltage. Assuming the gain is proportional to voltage through decrease in electron transit time, crystal A would have a gain of  $3 \times 10^3$  at 100 volts, which is more nearly like the values usually given.

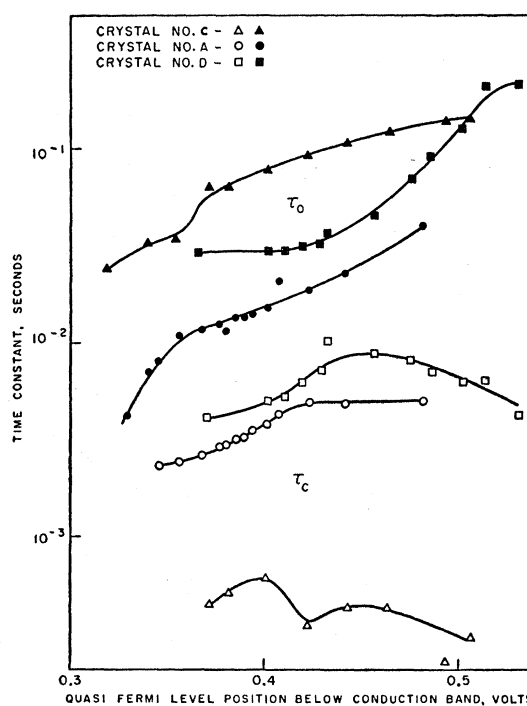


FIG. 2. Photoconductive decay constant,  $\tau_0$ , and conduction band lifetime  $\tau_c$  of CdS single crystals as a function of the position of the quasi-Fermi level below the conduction band and under 5200 Å illumination. Data for crystal B is not shown for clarity.

## III. PHOTOCONDUCTION NOISE

Van Vliet and Blok have shown that under certain assumptions the current noise density  $S_i$  of CdS single crystals with a single trap level may be expressed by<sup>3</sup>

$$S_i = \frac{4i^2}{n_0 V} \left\{ \frac{\langle \Delta n^2 \rangle}{n_0} \frac{\tau_0}{1 + \omega^2 \tau_0^2} + \frac{\tau_2}{\tau_0} \left[ (1 + \alpha) \frac{\tau_0}{\tau_c} - \frac{\langle \Delta n^2 \rangle}{n_0} \right] \frac{\tau_2}{1 + \omega^2 \tau_2^2} \right\} \quad (1)$$

where  $\langle \Delta n^2 \rangle$  is the variance of the conduction band electron density,  $\omega$  is the angular frequency,  $\tau_2$  is the relaxation time associated with the trap,  $\alpha$  is a constant describing the generation rate from traps, and the other terms have been previously defined. Equation (1) may be qualitatively understood as showing in the first term noise due to transitions from the system of conduction band and associated trap to the system of valence band and associated levels while the second term expresses the

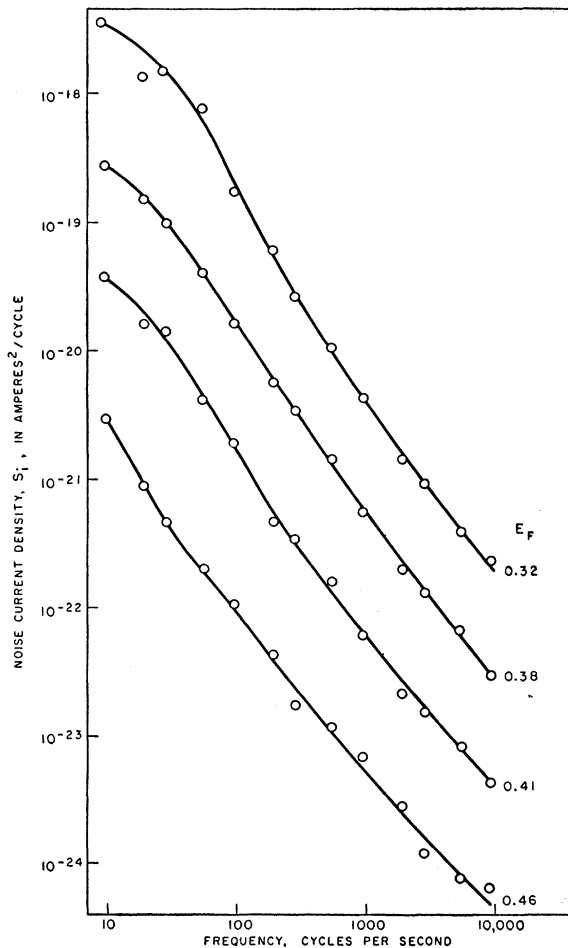


FIG. 3. Current noise spectra of crystal *A* at different 5200 Å illumination levels. The approximate  $1/f$  behavior at high frequencies should be noted.

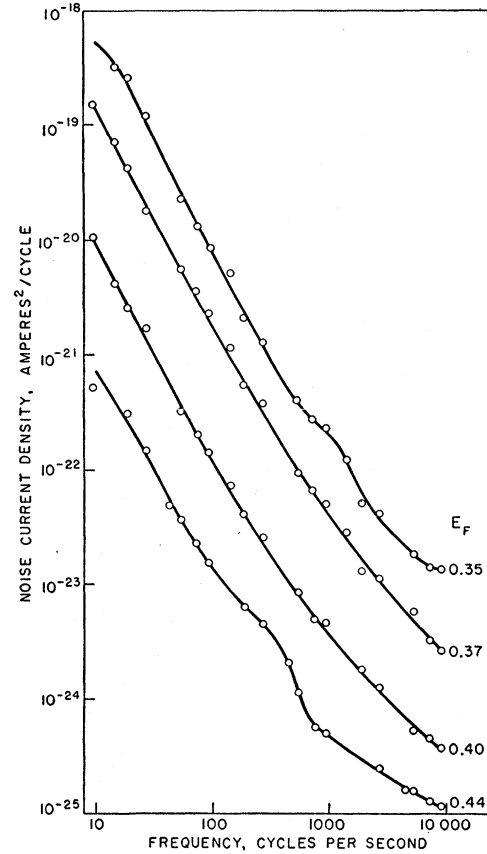


FIG. 4. Current noise spectra of crystal *B* at different 5200 Å illumination levels.

noise due to transitions within the first system. Measurements<sup>2</sup> show that the turnover frequency of the relaxation spectrum given by the first term is in good agreement with the photoconductive decay time as would be expected on this picture.

Current noise spectra at different illumination intensities for crystals *A*, *B*, and *C* are shown in Figs. 3, 4, and 5, and are qualitatively similar to those reported by Van Vliet. Crystal *A* exhibits a low-frequency relaxation spectra with a turnover below 10 cps and  $1/f$  noise at high frequencies which will be attributed to shallow trapping transitions. The low-frequency extent of the  $1/f$  noise component decreases as the quasi-Fermi level approaches the conduction band. Crystal *C* shows a similar low-frequency relaxation spectrum but little if any  $1/f$  noise is seen. Rather, a second relaxation process appears at 1750 cps when the quasi-Fermi level is near 0.41 volt below the conduction band. The spectra for crystal *B* appear to be intermediate between those of *A* and *C* in character. Qualitatively, these results suggest that the first term of Eq. (1) accounts for the major contribution to the observed spectra and that high-frequency fine structure is generated by the second term. The  $1/f$  noise in crystal *A* suggests a distribution of

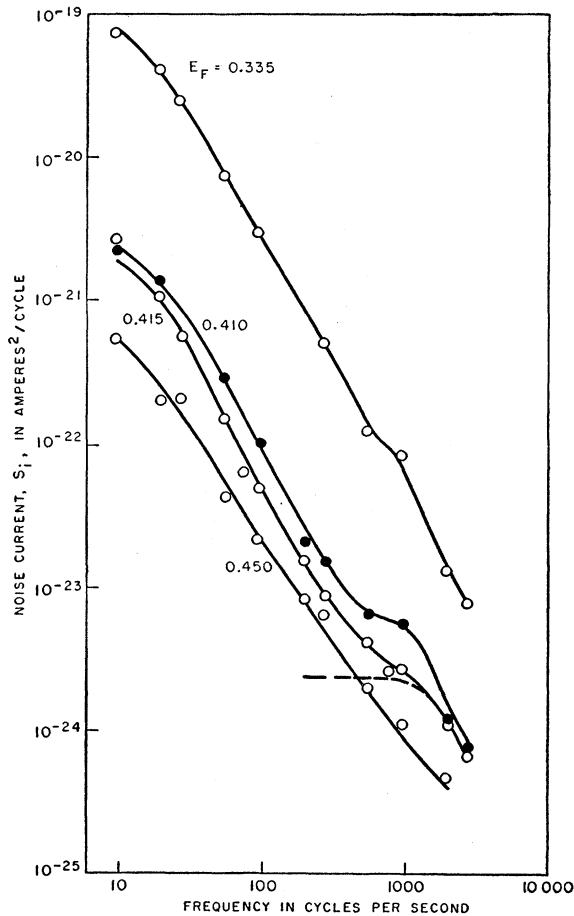


FIG. 5. Current noise spectra of crystal C at different 5200 Å illumination levels. The additional relaxation process at 1300 cps when  $E_F = 0.41$  volt is shown dotted.

trapping states in energy while the single process in crystal C implies a single dominating level near 0.4 eV below the conduction band.

When  $\omega\tau_2 < \omega\tau_0 < 1$ , that is, at low frequencies, Eq. (1) reduces to

$$S_i = (4i^2 \langle \Delta n^2 \rangle \tau_0) / n_0^2 V, \quad (2)$$

from which the total fluctuation,  $\langle \Delta n^2 \rangle / n_0$ , may be derived in terms of the experimental data. From variation of the noise with illumination, the magnitude of the carrier fluctuations with quasi-Fermi level position is determined as shown in Fig. 6. The open data points in the figure are for increasing illumination intensities while the solid data points are for decreasing intensities. The noise magnitude appears to be satisfactorily insensitive to illumination history. Further evidence for this is that the noise levels of Fig. 6 are in good agreement with those of Figs. 3, 4, and 5, which were taken several days apart and after much different illumination histories with regard to exposure to white light and time in the dark, etc.

Since it is expected that  $\langle \Delta n^2 \rangle / n_0 \sim 1$  for a Gaussian

process, the large values shown in Fig. 6 may imply that more electrons than those in the conduction band participate in the noise process. Following Van Vliet's suggestion,<sup>2</sup> these are assumed to be in shallow trapping levels and the data of Fig. 6 seems to be direct evidence for multiple retrapping in these levels.

#### IV. RETRAPPING

The observed low-frequency turnover corresponding to  $\tau_0$ , the increased noise magnitudes above that of photon noise and a simple recombination time, and the origin of fine structure can be interpreted by applying a simple retrapping model to Burgess's G-R theorem.<sup>4</sup> The model makes use of the fact that the hole lifetime is very short in CdS and hence that the contribution to the conductivity is negligible. Burgess derives an expression for the variance of  $n$  electrons in the conduction which is

$$\langle (n - n_0)^2 \rangle_{av} = \langle \Delta n^2 \rangle = \frac{g(n_0)}{r'(n_0) - g'(n_0)}$$

by solving the general equation

$$dP(n)/dt = r(n+1)P(n+1) + g(n-1)P(n-1) - [r(n) + g(n)]P(n),$$

where  $P(n)$  is the probability that there are precisely  $n$  electrons in the conduction band and  $g(n_0)$  is the generation rate of electrons into the conduction band when the steady-state concentration is  $n_0$ .  $r'(n_0) - g'(n_0) = (\partial r / \partial n)_{n_0} - (\partial g / \partial n)_{n_0}$  is a measure of the time to come to equilibrium when  $n \neq n_0$ .

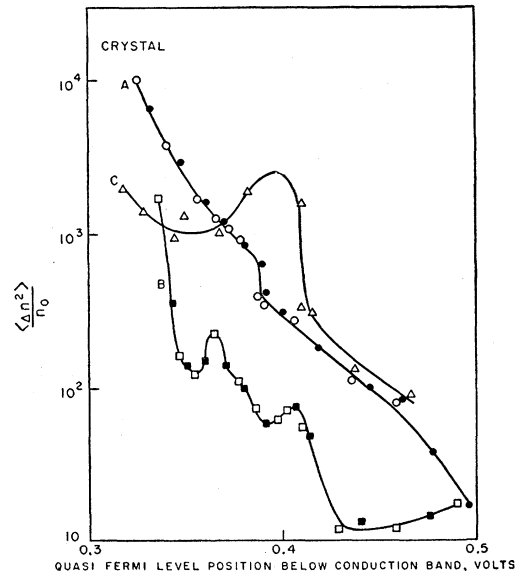


FIG. 6. Variation of the carrier fluctuations as a function of the quasi-Fermi level position. Open data points are for increasing illumination and solid data points are for decreasing illumination.

<sup>4</sup> R. E. Burgess, *Physica* **20**, 1007 (1954); also *Proc. Phys. Soc. (London)* **B69**, 1020 (1956).

If the intensity of the radiation is slightly changed, a new steady state concentration of electrons is reached after a time  $\tau_c$

$$\langle \Delta n^2 \rangle = g(n_0)\tau_c. \quad (3)$$

A well-known property of photoconductive insulators is that  $\tau_0$  is normally much larger than  $\tau_c$  except possibly at very high intensities of radiation, so that  $\tau_0$  and  $\tau_c$  can be considered to be related by

$$\tau_0 = \sum_{i=1}^m \tau_{ti} + \sum_{i=1}^{m+1} \tau_{ci} = \tau_t + \tau_c. \quad (4)$$

That is, an electron in the conduction band is bound after a time  $\tau_{ci}$  and is subsequently released back to the conduction band in a time,  $\tau_{ti}$  from the bound or trapped state.  $\tau_t$  is the total trapped time.

This process repeats  $m$  times, on the average, or until,

$$\sum_{i=1}^{m+1} \tau_{ci} = \tau_c,$$

at which time it disappears through recombination. The total average time which elapsed since initial generation by photon absorption is measured by the decay constant. However, the generation rate into the conduction band is now the sum of the photoexcitation rate,  $n_L = (n_0/\tau_c)$ , plus the excitation rate from the trap states. This rate may be expressed as the ratio of the total number of electrons in the traps,  $h_0$ , divided by the average time in the traps. Therefore,

$$g(n_0) = n_0/\tau_c + m h_0/(\tau_0 - \tau_c). \quad (5)$$

Similarly, the rate of disappearance of electrons from the conduction band,  $r(n_0)$ , is the ratio of the number in the conduction band divided by the average time in the conduction band, or

$$r(n_0) = (m+1)n_0/\tau_c. \quad (6)$$

Under steady-state conditions  $g(n_0) = r(n_0)$ , so  $h_0$  may be expressed in terms of the photoconductive experimental data as

$$h_0 = n_0(\tau_0 - \tau_c)/\tau_c. \quad (7)$$

Combining Eqs. (5), (6), and (3) yields

$$\langle \Delta n^2 \rangle / n_0 = (m+1) \quad (8)$$

which may be used to determine the average number of trapping transitions  $m$  from the experimental noise measurements.

The total electron concentration in traps and the average number of trapping transitions are shown in Figs. 6 and 7. The trapped electron density increases as the quasi-Fermi level rises, as does the number of transitions. In particular, Fig. 6 indicates that an electron may make several thousand transitions before recombining. Equations (7) and (8) show how photoconductivity data and noise measurements lead to information about the presence of traps and trapping kinetics, respectively.

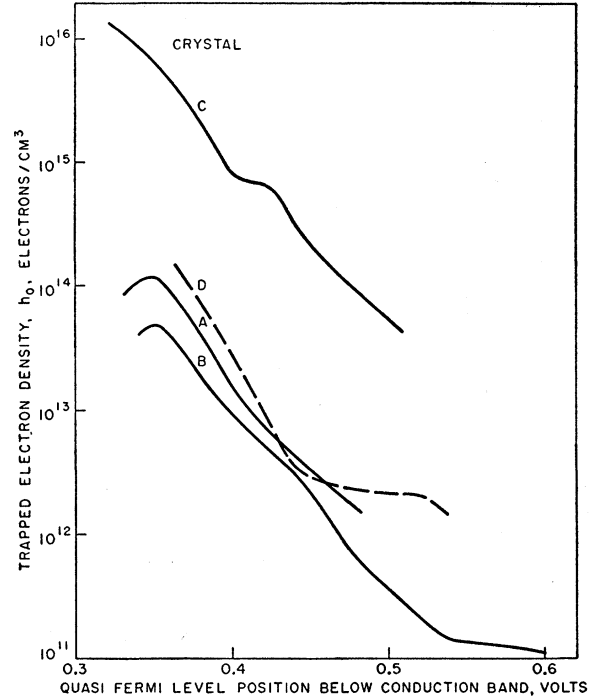


FIG. 7. Variation of the total concentration of electrons in traps.

In addition, however, to the steady-state generation and recombination rates from shallow traps which helps to account for the noise magnitude at the low-frequency end of the power density spectrum, there are fluctuations in the individual capture and release times. The fine structure of the power density spectrum can be interpreted on this model as fluctuation in these average times, which accounts for the departure from the simple  $1/f^2$  relationship at high frequencies.

## V. TRAP DENSITY AND FREQUENCY FACTOR

The energy distribution of trapping levels may be expressed in terms of the photoconductive observables by computing approximately the total number of electrons in traps:

$$h_0(E_F) = \int_0^{E_G} N_t(E) f(E, E_F) dE, \quad (9)$$

where the zero of energy has been taken at the top of the valence band,  $E_G$  is the forbidden bandwidth,  $N_t(E)$  is the energy density of traps at  $E$ ,  $f(E, E_F)$  is the Fermi function,  $E_F$  is the quasi-Fermi level, and the functional dependence of  $h_0$  has been indicated. This approach assumes that the coefficient of the exponential in the Fermi function is unity, which while not quite accurate for simple traps,<sup>5</sup> is sufficiently good for present purposes.<sup>6</sup>

<sup>5</sup> E. Spenke, *Electronic Semiconductors* (McGraw-Hill Book Company, Inc., New York, 1958), p. 387.

<sup>6</sup> J. R. Haynes and J. A. Hornbeck, *Photoconductivity Conference* (John Wiley & Sons, Inc., New York, 1956), p. 336.

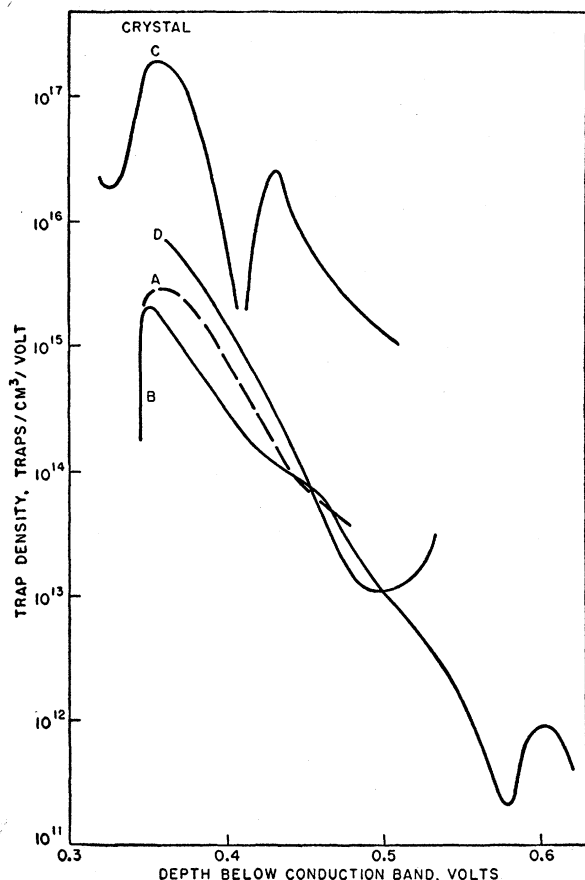


FIG. 8. Energy distribution of traps in Cds crystals.

Integral equation (9) may be formally solved if  $h_0(E_F)$  is known over the entire range of the definite integral, but present experimental data are available only for a limited part of the range. An approximate solution is obtained by differentiating both sides of (9) with respect to  $E_F$  and observing that  $\partial f / \partial E_F$  is strongly peaked at  $E = E_F$ . It is assumed that the major contribution to the integral comes at this point and  $N_t(E)$  is taken out from under the integral sign as  $N_t(E_F)$ . Thus  $N_t(E_F) = dh_0/dE_F$ , which by Eq. (7) becomes

$$N_t(E_F) = \frac{n_0}{kT} \left( \frac{\tau_0}{\tau_c} - 1 \right) + n_0 \frac{d}{dE_F} \left( \frac{\tau_0}{\tau_c} \right), \quad (10)$$

where  $k$  is Boltzmann's constant and  $T$  is the absolute temperature.

Rose<sup>1</sup> has suggested a solution to (9) which is essentially the first term of (10) and therefore (10) may be looked on as an improved solution. However, the value of the second term in (10) is comparable to the first, so that it is not a small correction. For example, apart from the factor  $(1/kT)$ , the first term is plotted in Fig. 7, which thus represents  $N_t(E)$  using Rose's solution, and

agrees with other such presentations.<sup>7</sup>  $N_t(E)$  derived from Eq. (10) and plotted in Fig. 8 shows marked departures from Fig. 7.

Figure 8 indicates levels at 0.36 and 0.60 eV which have been observed in thermally stimulated current experiments<sup>8</sup> on pure crystals. In addition, crystal C shows a strong level at 0.43 eV which is not so dominant in the others but which agrees with the spectra for this crystal as discussed in Sec. III. The trap density for crystal B shows a slight tendency for a concentration of levels at 0.44 eV. Samples A, B, and D also have a near exponential distribution of traps below 0.36 eV. Because of the success of Eq. (10) in deriving discrete levels in good agreement with results from thermally stimulated currents, it appears that this is a considerably more satisfactory way to obtain  $N_t(E)$  from photoconductivity data than that previously used.

Following the same technique, the generation rate from traps may be written as, using Eqs. (5) and (7),

$$mn_0/\tau_c = \int_0^{E_G} N_t(E) P(E) f(E, E_F) dE, \quad (11)$$

where  $P(E)$  is the trap escape probability of the traps at  $E$ . Here again the integral equation may only be solved in approximation and the same procedure used for Eq. (9) is followed. This leads to

$$P(E_F) = S(E_F) \exp \left( -\frac{E_G - E_F}{kT} \right) \\ = \frac{N_c}{N_t(E_F)} \left[ \frac{1}{kT} \left( \frac{m}{\tau_c} \right) + \frac{d}{dE_F} \left( \frac{m}{\tau_c} \right) \right] \\ \times \exp \left( -\frac{E_G - E_F}{kT} \right), \quad (12)$$

where  $N_c$  is the conduction band state density, and the usual exponential form for  $P(E)$  is derived directly by this technique.  $S(E)$ , the frequency factor, is thus the coefficient of the exponential on the right side.

Calculations according to (12) are presented in Fig. 9. In crystal A the frequency factor of the traps appears to be constant, which may indicate all these traps have the same origin. The frequency factor of crystal C approaches that of A near the position of the 0.41-eV discrete level. This may be an indication that this discrete level is structurally the same as the distributed levels in crystal A, which is qualitatively in agreement with the known impurity concentrations of the two crystals. A peak in the  $S(E)$  curve at 0.41 eV is also found for crystal B. The agreement in magnitude of  $S(E)$  at this point for the three crystals should be noted in view of the large differences in trap densities and noise magnitudes shown previously.

<sup>7</sup> H. B. DeVore, RCA Rev. **20**, 79 (1959).

<sup>8</sup> R. H. Bube, J. Chem. Phys. **23**, 18 (1955).

It is tempting to interpret these results as evidence for the same trap origin in all three specimens which tends to be at a discrete energy in the lightly doped crystals and broadens to an exponential distribution in more heavily doped crystals. A sufficiently reliable spectrochemical analysis is not presently available to quantitatively support this picture. It is interesting to note that the frequency factor of the 0.36-eV traps appears to be a strong function of impurity content. The magnitude of the frequency factors here derived are considerably greater than those obtained from thermally stimulated current results<sup>8</sup> but such data are notoriously difficult to analyze accurately. Noise measurements do not suffer from the same restrictions.

The approximations introduced in obtaining Eqs. (10) and (12), together with the errors inherent in graphical differentiation of experimental data, makes this analysis somewhat uncertain, particularly in the case of crystals *B* and *C*. For example, the maxima near 0.4 eV in Figs. 8 and 9 do not fall at the same place, as intuitively it seems they should. Assuming that only two discrete states, located at 0.36 and 0.43 eV (Fig. 8) are active in crystal *C*, it is possible to carry out an analysis similar to that represented by Eqs. (9) and (11) to determine the trap concentrations and frequency factors. This results in  $3.4 \times 10^{13}$  traps/cm<sup>3</sup> at 0.43 eV and  $8.5 \times 10^{15}$  traps/cm<sup>3</sup> at 0.36 eV and frequency factors in substantial agreement with those of Fig. 9. Since this discrete state technique does not employ the approximations leading to Eqs. (9) and (12), except in suggesting the presence of discrete states through Fig. 8, this agreement seems to lend support to the validity of the approximations introduced.

## VI. RETRAPPING NOISE

The preceding analysis arises from a knowledge of the carrier fluctuations determined only from low frequency noise measurements interpreted in terms of the first

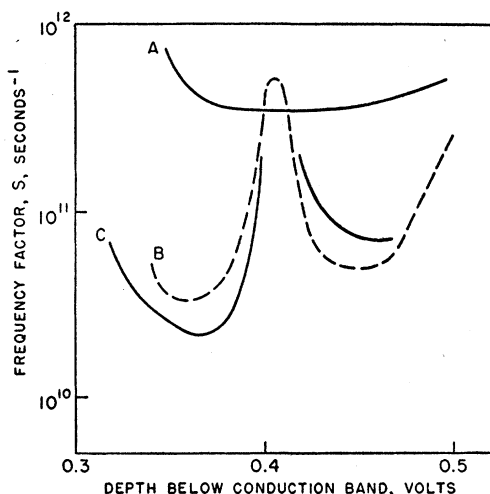


FIG. 9. Frequency factor of traps in CdS crystals.

term in Eq. (1). The noise spectra in Figs. 3 and 5 display additional features at high frequencies which are attributed to details of transitions between the traps and the conduction band as represented by the second term of Eq. (1). If this picture is correct the trap distributions and frequency factors presented above should be able to account for the remaining features of the spectra.

In Fig. 5 a single relaxation process is observed when the quasi-Fermi level is near 0.4 eV below the conduction band which is at the position of a maximum in the trap density shown in Fig. 8 and as derived from photoconductivity measurements alone. It is tempting to associate the relaxation time derived from the turnover frequency in the spectra,  $9 \times 10^{-5}$  second, with transitions to this nearly discrete level. From the G-R theorem, the ratio of the total low frequency noise to the trapping noise is  $\tau_0 \tau_c / \tau_2^2$  if the generation rate from traps dominates. Using the values given this ratio is  $3.6 \times 10^3$  compared to that observed in Fig. 5 of  $5 \times 10^3$ .

Also, the frequency factor should be of the order of  $\sigma v N_c$  where  $\sigma$  is the trapping cross section and  $v$  is the electron thermal velocity. Taking  $4 \times 10^{11}$  sec<sup>-1</sup> for  $S$  from Fig. 9 and a thermal velocity of  $10^7$  cm/sec, the calculated cross section is of the order of  $4 \times 10^{-15}$  cm<sup>2</sup>, which seems to be a reasonable value for neutral trapping. The spectra show the extra relaxation process only when the quasi-Fermi level is in the vicinity of the trap level which is qualitatively understandable in terms of electron population in the level.

The high-frequency portion of the spectra of crystal *A* show a  $1/f$  noise behavior which is also attributed to retrapping. It has been suggested a number of times that by superimposing spectra of the form  $\tau(1 + \omega^2 \tau^2)^{-1}$  with the time constants distributed proportional to  $1/\tau$ , a  $1/f$  spectrum results. It may be shown<sup>9</sup> that an exponential energy distribution of identical states can lead to  $1/f$  noise on this picture. The trap distribution for crystal *A* has a near exponential distribution below 0.36 volt. Furthermore, the average slope of this portion of the curve (Fig. 8) is  $-38$  volts<sup>-1</sup>, which is the proper value to obtain a  $1/f$  spectrum at room temperature. The constancy of the frequency factor (Fig. 9) at  $3 \times 10^{11}$  sec<sup>-1</sup> for these states is also a necessary requirement satisfactorily fulfilled.

The  $1/f$  spectrum is generated only by those traps above the quasi-Fermi level,<sup>9</sup> which means that as the quasi-Fermi level is raised, the low-frequency limit of the  $1/f$  behavior should move to higher frequencies. Qualitatively, the deeper traps have smaller transition probabilities, which implies slower relaxation times and as contributions are eliminated the lower frequency transitions are reduced. It is expected therefore that a

<sup>9</sup> A. L. McWhorter, *Semiconductor Surface Physics* (University of Pennsylvania Press, Philadelphia, Pennsylvania, 1957), p. 213; also published as Lincoln Laboratory Technical Report No. 80, Massachusetts Institute of Technology, Cambridge, Massachusetts, 1955).

TABLE II. Observed and calculated lower limit of  $1/f$  noise in crystal.

$E_F$ volts	$f_L$ cps	$P$ sec <sup>-1</sup>	$(P/2\pi)/f_L$
0.32	1200	$3.2 \times 10^5$	42
0.38	500	$3.0 \times 10^4$	9.7
0.41	200	$9.3 \times 10^3$	7.4
0.46	50	$1.4 \times 10^3$	4.5

correlation between the quasi-Fermi level position and the low-frequency appearance of  $1/f$  noise exist, as is observed in Fig. 3.

The approximate frequency of such a cutoff may be obtained for each of the spectra of Fig. 3 by extrapolating the low-frequency  $1/f^2$  trend to the intersection with extrapolation of the high-frequency  $1/f$  behavior. As shown in Table II, this intersection point indeed proceeds to higher frequencies as the quasi-Fermi level approaches the conduction band. Assuming that the turnover frequency associated with traps at the quasi-Fermi level is proportional to the trap escape probability divided by  $2\pi$ , the ratio of this frequency to the observed cutoff frequency is computed and shown in Table II. The ratio appears to be roughly constant and of the order of 10. Thus, there is at least semiquantitative experimental evidence for the exponential state distribution leading to  $1/f$  noise, a matter of some interest in the general problem of  $1/f$  noise in semiconductors.

It should, of course, be possible to account even more quantitatively for the spectra in terms of trapping transitions and there is some evidence in the present data that this is possible. While the average slope of the trap distribution is  $-38$  volts<sup>-1</sup>, there is a break in the curve at 0.44 volt shown in Fig. 8. Correspondingly, the noise spectra of Fig. 3 indicate that the high-frequency portions are more nearly  $1/f$  at high light intensities when the quasi-Fermi level is above this position. It appears

that more detailed interpretation must await more reliable data on the trap distribution than those achieved by the present technique. One wonders if the proper slope to account for  $1/f$  noise is fortuitous agreement, if the method used to derive the trap distribution prejudices the results to this value since the measurements are taken at room temperature, or if the kinetics of the trapping processes automatically lead to these results. Clearly, repetition of these measurements at lower temperatures should help answer these questions.

### VIII. SUMMARY

Through the use of combined current noise and photoconductivity measurements, it is thus possible to derive a coherent picture of transitions between the conduction band and shallow traps in single crystal cadmium sulfide. In particular, values for trap frequency factors can be obtained under steady-state conditions which appear more reliable than those realized from thermal stimulation experiments. Furthermore, the noise measurements appear to be direct evidence for multiple retrapping.

In this analysis electrons are presumed to recombine only from the conduction band and to communicate with other trapping states only through the conduction band. Extension of the analysis to allow such transitions directly would seem to be warranted. However, it seems that quantitative comparison with experiment must await more reliable determination of the trap distributions. To this end experiments at low temperatures are highly desirable.

It has been demonstrated semiquantitatively that the  $1/f$  noise component is due to an exponential distribution of identical traps, a matter of some interest in the general problem of  $1/f$  noise in semiconductors. Here again it seems that a completely satisfactory quantitative agreement must await more precise information about the trap distribution.